Available online at www.sciencedirect.com
SCIENCE DIRECT®
New Astronomy 11 (2006) 218–225
New Astronomy
www.elsevier.com/locate/newast

An astronomical site survey at the Barcroft Facility of the White Mountain Research Station

J. Marvil [a,b,*], M. Ansmann [a], J. Childers [a], T. Cole [c], G.V. Davis [a,c], E. Hadjiyska [a], D. Halevi [a], G. Heimberg [a], M. Kangas [a], A. Levy [a,b,d], R. Leonardi [a,e], P. Lubin [a,b], P. Meinhold [a,b], H. O'Neill [a,b], S. Parendo [a], E. Quetin [a], N. Stebor [a,b,d], T. Villela [e], B. Williams [a,b,d], C.A. Wuensche [e], K. Yamaguchi [a]

[a] *Department of Physics, University of California, Santa Barbara, CA 93106, United States*
[b] *UCSB Center for High Altitude, Astrophysics at White Mountain, University of California, Santa Barbara, CA 93106, United States*
[c] *College of Engineering, University of California, Santa Barbara, CA 93106, United States*
[d] *White Mountain Research Station, 3000 E. Line Street, Bishop, CA 93514, United States*
[e] *Instituto Nacional de Pesquisas Espaciais, Divisão de Astrofísica, Caixa Postal 515, São José dos Campos, SP 12210-070, Brazil*

Received 3 June 2005; accepted 16 June 2005
Available online 27 July 2005

Abstract

We present a distillation of weather and sky condition data collected from September 2001 to November 2004 at the University of California White Mountain Research Station, Barcroft Facility. Our conclusion is that Barcroft is an excellent site for microwave observation because of a cold microwave zenith temperature, low precipitable water, and a high percentage of clear days. The solar intensity was above 80% of the theoretical maximum 66% of the time. About 71% of the daytime, the cloud cover was acceptable for observing. Median precipitable water vapor was estimated to be 1.75 mm. We measure a median opacity at 225 GHz of 0.11, which corresponds to a transmission of 89.6%. Zenith sky temperatures were determined to be 9.0 ± 0.2 K and 10.0 ± 0.6 K in Q-band (38–46 GHz) and W-band (81–98 GHz), respectively. We also demonstrate a correlation between measurements of precipitable water vapor from a weatherstation and a 225 GHz radiometer.

Keywords: Site testing; Atmospheric effects; Cosmic microwave background

* Corresponding author. Tel.: +1 805 893 8418; fax: +1 805 893 8498.
E-mail address: marvil@deepspace.ucsb.edu (J. Marvil).

1384-1076/$ - see front matter © 2005 Elsevier B.V. All rights reserved.
doi:10.1016/j.newast.2005.06.005

1. Introduction

The University of California, Santa Barbara (UCSB) Center for High Altitude Astrophysics at White Mountain has been observing from the Barcroft facility of the University of California White Mountain Research Station (WMRS) since 2001. Barcroft was chosen for its high elevation, good infrastructure, and relatively close proximity to UCSB. Along with the deployment of millimeter wave telescopes, several instruments have been installed to monitor weather and sky conditions. These serve to characterize the site and aid in the data selection and remote operation of our telescopes. A commercial weather station is used to measure temperature, humidity, barometric pressure, solar intensity, and wind speed. An optical monitor archives images of the sky, which are rated according to the amount of cloud cover. Atmospheric opacity at 225 GHz has been measured by a NRAO tipper. Furthermore, zenith sky temperatures have been measured by the WMPol (Levy et al., 2005) telescope, which is a dedicated instrument for measuring polarization of the Cosmic Microwave Background.

2. Site description

WMRS Barcroft is located in the White Mountains east of Bishop, CA at 37°35′ N Latitude; 118°15′ W Longitude and 3.8 km in elevation. Barcroft is accessible by car via a partially unpaved road while snow conditions permit. Otherwise, access is limited to SnoCat. The Internet is available from a redundant configuration of a commercial satellite dish[1] and a wireless extension[2] of the network at the WMRS Owens Valley Laboratory. The facility accommodates a wide breadth of research including but not limited to astronomy, astrophysics, atmospheric science, physiology, biology, geology, ecology, botany, and alternative energy.

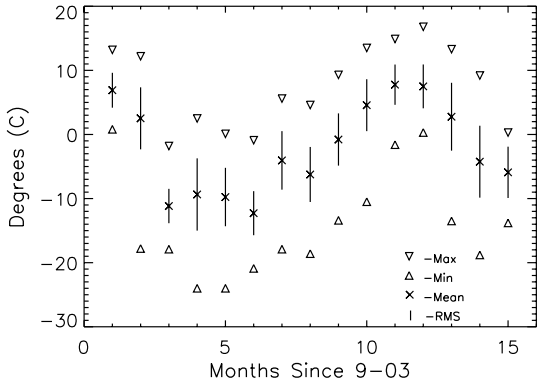

Fig. 1. Temperature statistics by month from September 2003 to November 2004.

3. Weather station

A commercial weather station[3] was deployed at Barcroft in September 2001 and a second identical one outside the observatory dome in September 2003. These record temperature, humidity, wind speed, wind direction, and barometric pressure. A solar intensity monitor was added to the observatory dome sensor package in March 2004. WMRS hosts a webpage[4] that links to data from these stations and several other sources. We have analyzed a near-continuous archive of 10-min samples from the observatory dome station, which is summarized below.

3.1. Temperature

Between September 2003 and November 2004, the average temperature was −2.2 °C with a maximum of 16.8 °C and minimum of −24 °C. The mean daily high–low temperature swing was approximately 8 °C. Fig. 1 shows the monthly high, low, mean, and standard deviation.

3.2. Wind speed

The weather station records both a 10-min average and 10-min peak wind speed. The average wind speed throughout our archive is 11.2 mph.

[1] http://www.starband.com
[2] http://www.wi-lan.com
[3] http://www.davisnet.com
[4] http://www.wmrs.edu/weather

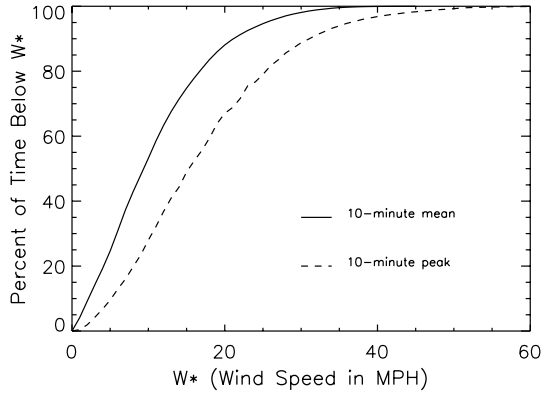

Fig. 2. Cumulative distributions for high and mean wind speeds from September 2003 to November 2004. The maximum peak wind speed for this time period was 76 mph.

The highest recorded instantaneous wind speed was 76 mph. We determine that 11% of the time the peak wind exceeds 30 mph in a 10-min period. A cumulative distribution (integrated histogram) of average and peak wind speed is shown in Fig. 2. For comparison, the Mauna Kea VLBA site experienced median wind speeds of 10.1 mph with a maximum of 64 mph between May, 1995 and April, 1996 (Holdaway et al., 1996). For the same duration, wind speeds at Chajnantor, Chile had a median of 13.4 mph and high of 73 mph (Holdaway et al., 1996).

3.3. Solar irradiance

The solar radiation sensor consists of a silicon diode (sensitive between 300 and 1100 nm) mounted horizontally with a diffusing window. The sensor is very responsive to clouds passing in front of the sun. Fig. 3 shows the effect of cloud cover on the solar sensor by comparing an adjacent clear and cloudy day. From this sensor data we estimate the number of clear days at Barcroft. First we integrate the total solar intensity for each day. Clear days are selected and used to model the variation in solar intensity throughout the year. All days are then compared to this model and their percent deviation is calculated. Fig. 4 shows the a histogram of the percent deviation. For instance, 66% of the days the solar radiation was at least 80% of the predicted maximum.

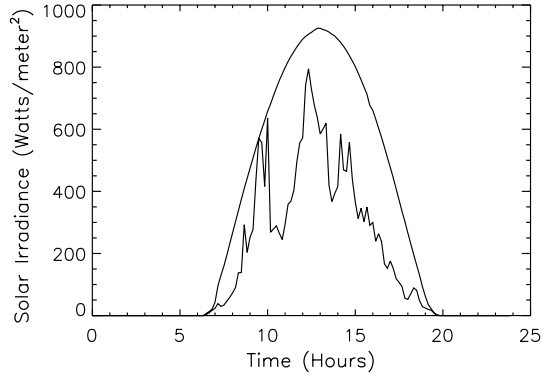

Fig. 3. Signals from the solar irradiance monitor. A sample clear and cloudy day are overplotted for comparison.

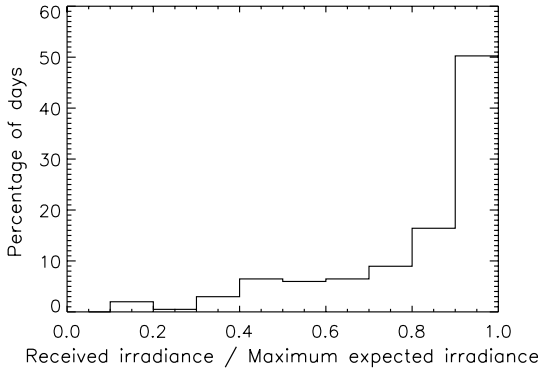

Fig. 4. Histogram of daily solar irradiance as a fraction of the expected maximum. This was measured over the period March, 2004 to November, 2004.

4. Cloud cover

A USB webcamera[5] was deployed to monitor a $30° \times 40°$ patch of sky near the north celestial pole. This camera delivers live video in 640×480 resolution and captures 1024×768 stills. Live video is primarily used for remote operations. The stills are archived and analyzed for cloud cover from which we estimate the percentage of clear days. Daytime images were manually rated with a score of 1–4: '1' completely clear, '2' clouds cover less than 50% of the sky, '3' clouds cover more than 50% of the sky, and '4' completely overcast. The

[5] http://www.creative.com

Table 1
A cloud cover analysis of optical images taken during daylight hours between October 2003 and November 2004

Clear	41.8%
Partly cloudy	29.7%
Mostly cloudy	14.1%
Overcast	14.4%

distribution is shown in Table 1. An automated image-processing algorithm developed to produce this rating is presented in Kangas et al. (2005).

Cloud cover has a tremendous impact on the performance of astrophysical observations. We show that the degree of cloud cover is well correlated with WMPol's time ordered data. The sensitivity of the telescope can be estimated from the rms of the raw data; a high rms denotes poor instrument performance. The rms of the WMPol data were calculated in 20-min intervals and binned according to the degree of cloud cover present at the time of observation. Fig. 5 compares the W-band (81–98 GHz) and Q-band (38–46 GHz) rms to the degree of cloud cover. Both the mean and standard deviation are shown to increase as the sky becomes more cloudy.

We conclude the sky is acceptable for observing when the score is 1 or 2. Over the archive period of October 2003 to November 2004, 71% of the time the sky was determined to be acceptable. This is consistent with the fraction of clear sky derived from the solar irradiance and is on par with other sites. The yearly percentage of observable nights was found to be 67% on Mauna Kea, 82% at La Silla and Cerro Tololo, and 75% for Las Palmas (ESPAS, 2003).

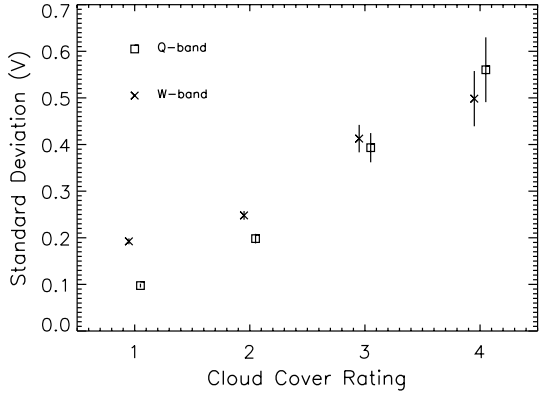

Fig. 5. Correlation of the mean RMS of WMPol's Q-Band and W-Band Data Acquisition Channels with the Cloud Cover Rating. The vertical lines represent the standard deviation. In both cases, both the mean signal rms and the standard deviation increase with increasing cloud cover.

5. Microwave sky temperature

As the pointing of a telescope deviates from zenith the column of foreground air mass increases, which causes a rise in sky brightness temperature. In the simple model that the atmosphere is an infinite flat slab of constant density, this signal varies as the secant of the elevation angle.

The WMPol telescope preformed several sky dips from 32° to 49° elevation. These data were calibrated and applied to the flat slab model to fit for zenith temperature and instrument noise. We measured mean zenith temperatures of 9.0 ± 0.2 K in Q-band and 10.0 ± 0.6 K in W-band. The uncertainty represents the standard deviation of the distribution of sky temperatures measured on optically clear days.

We have developed an atmospheric modeling program (hereafter called ATMOS) to estimate sky brightness and opacity as a function of frequency. ATMOS uses a standard US atmosphere temperature–pressure profile and pressure-broadened emission by H_2O, O_2, and O_3 as referenced

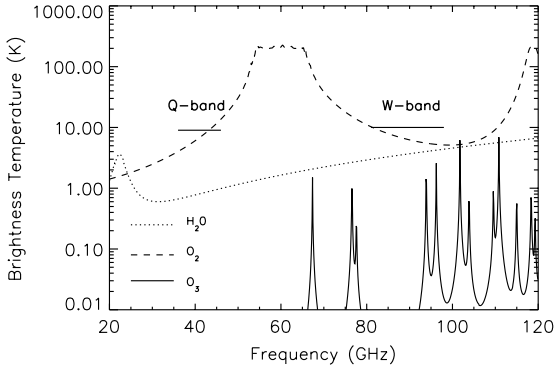

Fig. 6. A model of the sky temperature resulting from H_2O, O_2, and O_3 for a sea-level water vapor density of 10 g/m^3. The two horizontal lines are drawn between the 3db points of the Q- and W-Band band passes at a level corresponding to their measured sky temperature.

from a Jet Propulsion Laboratory line catalog. Fig. 6 shows the results of this simulation for a sea-level water vapor density of 10 g/m^3, which is a good fit to our measured sky temperatures.

6. Atmospheric opacity

The NRAO Tipper is a 225 GHz radiometer (McKinnon, 1987) that measures sky signal as a function of elevation angle. It uses a temperature-stabilized blackbody to obtain a calibrated atmospheric opacity, τ. At 225 GHz, opacity is dominated by H_2O as shown in Fig. 7. We measured a median τ_{225} of 0.11 for 50 days between September, 2001 and November, 2001 (quartiles: 25% 0.077, 50% 0.112, 75% 0.155). Fig. 8 shows the cumulative histogram of τ_{225}, and Fig. 9 shows the opacity as a function of hour in local time. This shows that the sky is most opaque between 5 p.m. and 8 p.m.

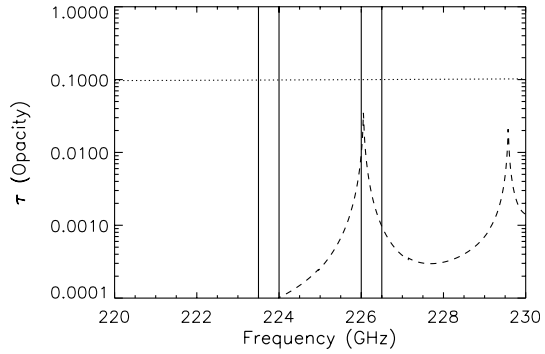

Fig. 7. An ATMOS simulation of atmospheric opacity τ for H_2O (dotted) and O_3 (dashed) using a troposphere water content of 10 g/m^3. The contribution from O_2 is below 10^{-4}. The dual band passes of the tipper are shown with vertical lines between 223.5–224 and 226–226.5 GHz. Note the presence of an ozone line in the upper sideband.

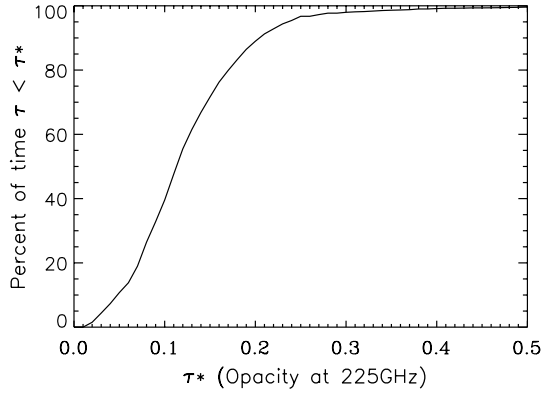

Fig. 8. Cumulative distribution of the optical opacity, τ, measured with a 225 GHz NRAO tipper between September 2001 and November 2001.

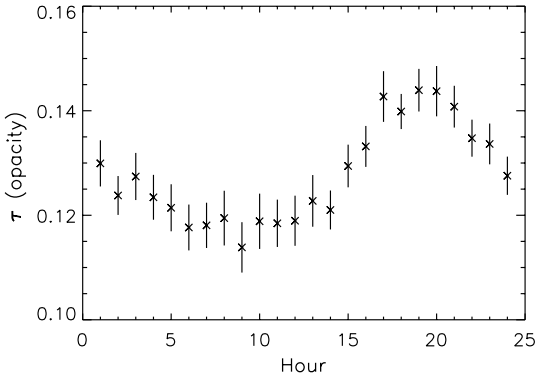

Fig. 9. Optical opacity, τ, measured with a 225 GHz NRAO tipper between September 2001 and November 2001, binned by hour of the day.

7. Precipitable water

Precipitable water vapor (PWV) is a measure of the total water contained in a vertical column above the site. It is commonly expressed as the resulting height of liquid water if all the vapor in the column were condensed. ATMOS was used to calculate this height, l_{pwv}, at 3.8 km for a range of sea-level water vapor density ρ_0. A linear fit of PWV vs. ρ_0 is given in Eq. (1):

$$l_{\mathrm{pwv}} = 0.174\rho_0, \tag{1}$$

where l_{pwv} is precipitable water vapor in mm and ρ_0 is sea-level water vapor density in g/m^3. By varying ρ_0 and integrating over the bandpass of the tipper, we find a linear relationship between τ_{225} and l_{pwv}. Eq. (2) best fits this data:

$$\tau_{225} = 0.0571 l_{\mathrm{pwv}} + 0.003. \tag{2}$$

Applying this relationship to the tipper data results in a median l_{pwv} of 2.05 mm.

Alternatively, the precipitable water at Barcroft has been estimated based on local temperature and humidity. Specifically, the Magnus Teten equation is evaluated at the dewpoint to determine the local vapor pressure of water (Murray, 1967). This is given by Eq. (3)

$$\log_{10} P_{\mathrm{vp}} = \frac{7.5T}{T + 237.3} + 0.7858, \tag{3}$$

where P_{vp} is the vapor pressure of H_2O in hPa and T is the dewpoint temperature in degrees Celsius.

This is used to estimate integrated l_{pwv} from an atmospheric model (Allen, 1973) as shown in Eq. (4)

$$l_{\mathrm{pwv}} = 2.1 P_{\mathrm{vp}}(h) 10^{-h/22}, \tag{4}$$

where h is the height in kilometers and $P_{\mathrm{vp}}(h)$ is the vapor pressure of H_2O in mmHg at height h.

Using dewpoint measurements taken concurrently with the tipper, we find a correlation between the two methods of estimating PWV. We divide the dewpoint and tipper measurements into corresponding 1-day and 1-h bins. To the dewpoint we apply (3) and (4), and to the tipper we apply (2). Fig. 10 shows the 1-day bins for each dataset, and Fig. 11 shows the correlation plot.

We fit a line to Fig. 11 with the constraint that it passes through the origin. From this we derive that the dewpoint analysis overestimates the PWV by 12%. Applying this to the entire archive of dewpoint measurements yields a median PWV of 1.97 mm, which is lower than during the 50 days of 2001. Fig. 12 shows a cumulative distribution of the results of this analysis. In 1995, Mauna Kea has been shown to have a median PWV of 2.2 mm (ESPAS, 2003).

This relationship can be applied to the entire dewpoint dataset, from September 2003 to November 2004. This produces a lower PWV averaged over the year than during the 50 days the tipper was operational. The yearly PWV quartiles are shown to be 1.15, 1.75, and 2.45 mm. We use

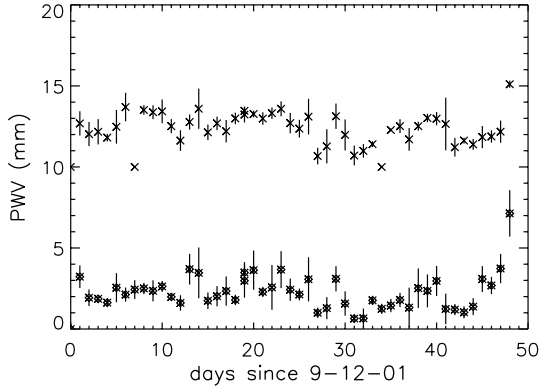

Fig. 10. Estimated PWV from 50 days of τ_{225} measurements and the corresponding 50 days of dewpoint measurements. The stars represent the daily mean of PWV derived from the tipper, and the Xs show the daily mean of PWV from the dewpoint, shifted up by 10 mm.

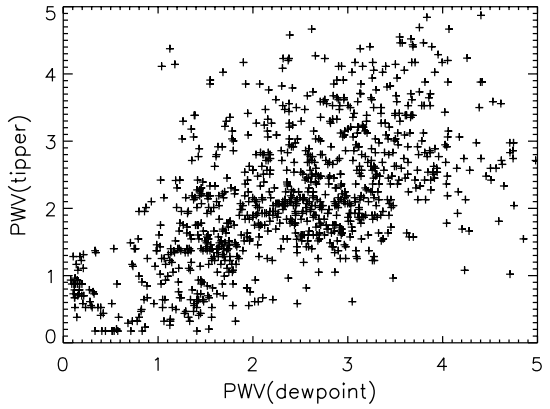

Fig. 11. Correlation plot between PWV estimated by dewpoint and PWV estimated by the tipper. Fitting a line constrained to pass through the origin shows that in general, the dewpoint analysis overestimates the tipper-determined value of PWV by 12%.

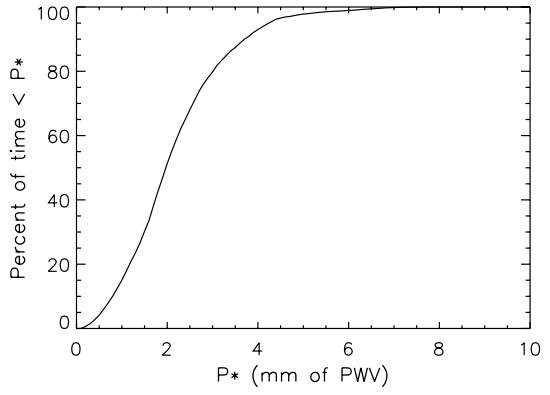

Fig. 12. Cumulative distribution of PWV derived from dewpoint measurements between September 2003 and November 2004. The values of PWV have been reduced by 12% in accordance with the correlation shown in Fig. 11.

Eq. (2) to estimate the yearly optical opacity quartiles. Table 2 shows these in comparison to other sites. Fig. 13 shows the zenith temperatures resulting from the 25% and 75% precipitable water quartile values and Fig. 14 shows the corresponding transmission ($e^{-\tau}$). Table 3 shows the opacity and sky brightness temperature in typical microwave band passes for the 25%, 50%, and 75% precipitable water quartiles.

Table 2
Quartiles for 225 GHz optical opacity, τ, from various sites

Location	τ 25%	τ 50%	τ 75%
WMRS Barcroft[a]	0.079	0.112	0.156
WMRS Barcroft[b]	0.069	0.103	0.143
CSO Mauna Kea	0.064	0.103	0.179
Chajnantor	0.036	0.061	0.115
South Pole	0.043	0.053	0.066

Note. Non-WMRS data were obtained from Radford and Chamberlin (2000).

[a] Measured with tipper for 50 days between September 2001 and November 2001.

[b] Estimation based on dewpoint.

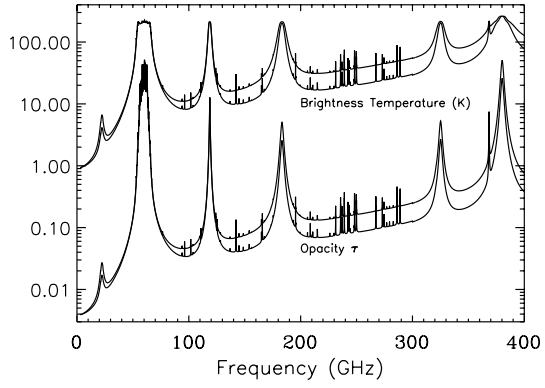

Fig. 13. Zenith sky brightness temperature (K) and Opacity τ for the 25% and 75% precipitable water quartiles.

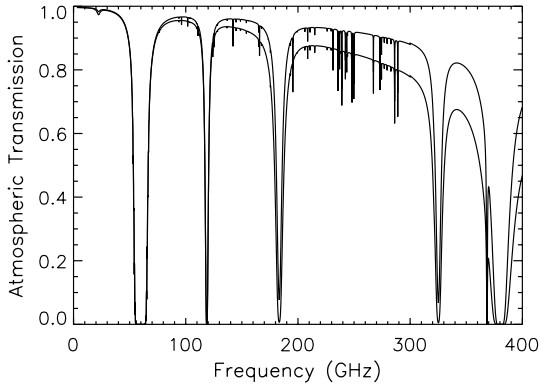

Fig. 14. Zenith transmission for the 25% and 75% precipitable water quartiles.

We also predict the transmission for other sites using the same atmospheric modeling code. Using median values we find that CSO and Barcroft are nearly identical. Fig. 15 compares the results for Barcroft, CSO, Chajnantor, and the South Pole.

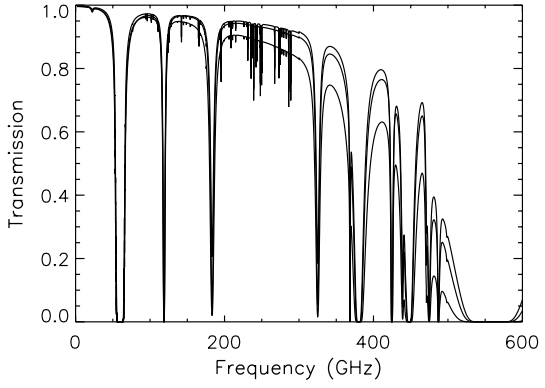

Fig. 15. Comparison of modeled atmospheric transmission for median PWV at different sites. The topmost curve is the South Pole, below that is Chajnantor and the lowest is Barcroft and Mauna Kea, which are nearly identical at the 50% quartile level.

Table 3
Predicted quartiles for atmospheric opacity and sky brightness temperature at various frequency intervals

Bandpass (GHz)	τ 25%	τ 50%	τ 75%	T_{sky} 25%	T_{sky} 50%	T_{sky} 75%
26–36	0.0134	0.0142	0.0153	3.22	3.41	3.68
38–46	0.373	0.0383	0.0396	8.77	9.01	9.34
81–98	0.0393	0.0436	0.0494	9.34	10.40	11.80
135–165	0.0457	0.0603	0.0797	11.12	14.60	19.14
198–242	0.0766	0.105	0.144	18.42	25.01	33.48
252–308	0.111	0.155	0.213	26.14	35.72	47.75
335–365	0.25	0.35	0.49	54.38	66.54	94.16

8. Conclusions

We find that 89% of the time the wind speed is low enough at WMRS to observe with WMPol. About 70% of the time the sky is relatively clear. Microwave sky brightness temperatures are low and well matched to a model with a median precipitable water vapor of 1.6 mm. This makes WMRS Barcroft an excellent site for millimeter-wave observations below 300 GHz. Furthermore, we have demonstrated that local humidity as measured by a weather station reasonably correlates with integrated water vapor as measured by a radiometer.

Acknowledgments

We would like to thank all the WMRS staff members involved with the Barcroft Facility for their invaluable assistance. Without them, this research would not have been possible. This work was funded by NASA grants NAG5-4078, NAG5-9073, and NAG5-4185, and by NSF grants 9813920 and 0118297. In addition we were supported by the White Mountain Research Station, the California Space Institute (CalSpace), and the UCSB Office of Research. R. Leonardi was supported by CAPES. A. Levy was supported by CalSpace Grant and the WMRS Graduate Research Fellowship. T. Villela and C.A. Wuensche were partially supported by FAPESP Grant 00/06770-2. In addition, T. Villela acknowledges support from CNPQ Grant 307433/2004-8-FA and FAPESP Grant 96/06501-4.

References

Allen, C.W., 1973. Astrophysical Quantities, 3rd ed. The Athlone Press, London, p. 120.

ESPAS Site Summary Series: Mauna Kea, Issue 1.2, June 2003 http://www.eso.org/gen-fac/pubs/astclim/espas/espas_reports/ESPAS-Maunakea.pdf.

Holdaway, M.A., et al., 1996. MMA Memo #159: Wind Velocities at the Chajnantor and Mauna Kea Sites and the Effect on MMA Pointing.

Kangas, M., et al., 2005, in preparation.

Levy, A., et al., 2005, in preparation.

McKinnon, M., 1987. MMA Memo #40: Measurement of Atmospheric Opacity Due to Water Vapor at 225 GHz.

Murray, F.W., 1967. J. Appl. Meteorol. 6, 203.

Radford, S.J.E., Chamberlin, R.A., 2000. MMA Memo # 334.1: Atmospheric Transparency at 225 GHz over Chajnantor, Mauna Kea, and the South Pole.